

Design of Directivity Patterns with a Unique Null of Maximum Multiplicity

Chao Pan, Jacob Benesty, and Jingdong Chen

Abstract—Differential beamforming is one of the most popular beamforming approaches, which has the great potential to form frequency-invariant directivity patterns. In this paper, we study the design of beampatterns with multiple nulls in the same direction, which is clearly different from the design of beampatterns with distinct nulls. Our contributions are as follows. First, we show how to constrain multiple nulls to the same direction and design the desired beampattern with both the traditional and robust approaches. Second, we derive an explicit form of the white noise gain (WNG) of the traditional approach as a function of the frequency, interelement spacing, and null direction, which shows that the cardioid is the optimal beampattern as far as the WNG is concerned. Third, we prove that the WNG improvement of the robust approach rarely depends on the null direction at low frequencies. Finally, considering the fact that the robust differential beamforming approach may produce a frequency-dependent beampattern while improving the WNG, we develop a weighted-norm approach that can make a good compromise between the robustness of differential beamforming with respect to white noise and the frequency-invariant beampattern. The performance of the developed approach is verified by simulations.

Index Terms—Beamforming, beampattern design, differential microphone arrays, directivity factor, microphone arrays, white noise gain.

I. INTRODUCTION

MICROPHONE arrays combined with wideband beamforming techniques have the potential to be widely used in all kinds of hands-free communication systems for speech enhancement, noise reduction, spatial sound recording, reverberation suppression, interference rejection, source localization, etc. Among different types of microphone arrays, the so-called differential microphone arrays (DMAs), which

consist of a set of closely-spaced sensors and differential beamforming, have attracted much research and development attention recently, thanks to their frequency-invariant beampatterns, high directivity factors (DFs), and small apertures [1]–[10].

The array gains of DMAs in a spherically isotropic noise field are usually much higher than those of uniform linear arrays with the same number of microphone sensors and the interelement spacing close or equal to the half wavelength; therefore, DMAs are often viewed as superdirective arrays [11]. Similar to other superdirective arrays, DMAs are also sensitive to the sensors' self noise and mismatch between sensors, particularly at low frequencies [3]. For the conventional superdirective arrays, the diagonal loading technique has been investigated for improving the robustness against uncorrelated errors among sensors [12], [13]; however, it was found to degrade significantly the DFs. With the traditional DMAs, which are implemented in a multi-stage (cascade) manner [4], there has been no effective way to improve the robustness with respect to sensors' self noise so far.

Recently, a framework was developed to design DMAs in the frequency domain [1], [9], which converts the DMA design problem into one of linear equation system solving. One of the most prominent properties of this approach is that it can improve the robustness of the DMA by increasing the number of sensors in the array while fixing the DMA order. This is achieved by maximizing the white noise gain (WNG) subject to some fundamental constraints from the desired (target) beampattern of a given order DMA. Since it can significantly improve the robustness of DMAs, depending on the number of sensors, this linear system solving approach is called the robust DMA design method. However, this robust approach is found to suffer from one problem: its beampattern becomes slightly frequency dependent, particularly at high frequencies where the designed beampattern may differ from the desired one.

In [10], the spatial \mathcal{Z} transform was introduced to study and analyze the robust DMA design approach. It was demonstrated that the robust approach to DMA beamforming can be divided into two cascaded filters: the first-stage filter forms the desired beampattern while the second-stage one improves the WNG. Through this decomposition, we can, on the one hand, get better understanding of the robust DMA design method, and on the other hand, develop new algorithms that can better deal with the two contradictory issues in DMA design: white noise amplification and frequency invariance of beampatterns.

Another way to form differential beamformers is through the use of a series expansion [14], [15]. Again, we can improve the robustness of the DMA by increasing the number of microphone sensors. However, this series-expansion method does not have

Manuscript received April 22, 2015; revised September 22, 2015; accepted November 28, 2015. Date of publication December 01, 2015; date of current version January 04, 2016. This work was supported in part by the NSFC "Distinguished Young Scientists Fund" under Grant 61425005. The work of C. Pan was supported in part by the China Scholarship Council. The associate editor coordinating the review of this manuscript and approving it for publication was Prof. Hiroshi Saruwatari.

C. Pan is with the Center of Intelligent Acoustics and Immersive Communications and School of Marine Science and Technology, Northwestern Polytechnical University, Xi'an 710072, China, and also with INRS-EMT, University of Quebec, Montreal, QC H5A 1K6, Canada (e-mail: panchao2nwpu@mail.nwpu.edu.cn).

J. Benesty is with INRS-EMT, University of Quebec, Montreal, QC H5A 1K6, Canada (e-mail: benesty@emt.inrs.ca).

J. Chen is with the Center of Intelligent Acoustics and Immersive Communications, Northwestern Polytechnical University, Xi'an 710072, China (e-mail: jingdongchen@ieee.org).

Color versions of one or more of the figures in this paper are available online at <http://ieeexplore.ieee.org>.

Digital Object Identifier 10.1109/TASLP.2015.2504866

much flexibility in controlling the null positions and the DMA beampattern.

In this paper, we focus on a particular class of beampatterns that have a unique null of maximum multiplicity. These beampatterns will be designed in the frequency domain [1] and analyzed with the two-stage framework [10]. The motivation of this work is as follows.

- There are no sidelobes in this class of beampatterns if the null is in the back part of the coordinate system, which is desired in many practical applications.
- The analysis and performance study of such beampatterns is easier, which can lead to a better understanding of DMAs.
- Both the dipole and the cardioid beampatterns, which are the two most important beampatterns that are widely used in practice, are special cases of this class.

The major contributions of this work are fourfold. 1) We show how to constrain multiple nulls to the same direction and design the desired beampattern with both the traditional and robust approaches. 2) We derive an explicit form of the WNG with the traditional approach as a function of the frequency, interelement spacing, and null direction, which shows that the cardioid has the highest WNG among other beampatterns. 3) We prove that the WNG improvement of the robust approach does not depend on the null positions, and this is particularly true at low frequencies. 4) Considering that the series-expansion methods in [14] and [15] cannot be used to design beampatterns with a unique null of maximum multiplicity and the robust approach in [1] and [9] may suffer from beampattern deformation, we develop a weighted-norm approach that can make a good compromise between the robustness of differential beamforming with respect to white noise and the frequency-invariant beampattern.

The rest part of this paper is organized as follows. In Section II, we present the signal model for beamforming in the frequency domain and give the performance measures. Section III discusses DMA beampatterns. In Sections IV and V, we focus on the design of beampatterns with the traditional and robust approaches, respectively. Meanwhile, we investigate their performance by means of beampattern, DF, and WNG. We show that the robust approach improves the WNG; but both the beampattern and the DF may be deformed. In Section VI, we derive a beamformer by maximizing the DF with the constraints on the desired beampattern. However, the resulting beamformer may have a frequency-dependent beampattern and sometimes even introduces extra nulls in the mainlobe side of the beampattern. To circumvent this drawback, we develop in Section VII a weighted-norm approach that can better compromise among the beampattern, DF, and WNG. Finally, some conclusions are given in Section VIII.

II. SIGNAL MODEL, PROBLEM FORMULATION, AND DEFINITIONS

We consider a desired source signal, in the farfield, that propagates from the azimuth angle, θ , in an anechoic acoustic environment at the speed of sound, i.e., $c = 340$ m/s, and impinges on a uniform linear array consisting of M omnidirectional microphones. The angular frequency is denoted by $\omega = 2\pi f$, where $f > 0$ is the temporal frequency. In this context, the

observation signal vector of length M can be expressed in the frequency domain as [16]

$$\begin{aligned} \mathbf{y}(\omega) &\triangleq [Y_1(\omega) Y_2(\omega) \cdots Y_M(\omega)]^T \\ &= \mathbf{x}(\omega) + \mathbf{v}(\omega) \\ &= \mathbf{d}(\omega, \cos \theta) X(\omega) + \mathbf{v}(\omega), \end{aligned} \quad (1)$$

where $Y_m(\omega)$ is the m th microphone signal, the superscript T is the transpose operator, $\mathbf{x}(\omega) = \mathbf{d}(\omega, \cos \theta)X(\omega)$, $X(\omega)$ is the desired source signal,

$$\mathbf{v}(\omega) = [V_1(\omega) V_2(\omega) \cdots V_M(\omega)]^T \quad (2)$$

is the additive noise signal vector with $V_m(\omega)$ being the noise at the m th microphone,

$$\begin{aligned} \mathbf{d}(\omega, \cos \theta) \\ \triangleq [1 \quad e^{-j\omega\tau_0 \cos \theta} \quad \cdots \quad e^{-j(M-1)\omega\tau_0 \cos \theta}]^T \end{aligned} \quad (3)$$

is a phase-delay vector of length M (which is the same as the steering vector used in traditional beamforming), $j = \sqrt{-1}$ is the imaginary unit, and $\tau_0 = \delta/c$ is the delay between two successive sensors at the angle $\theta = 0^\circ$, with δ being the interelement spacing.

To ensure that differential beamforming takes place, the following two assumptions are made [1], [4].

- 1) The sensor spacing, δ , is much smaller than the acoustic wavelength, $\lambda = c/f$, i.e.,

$$\omega\tau_0 \ll 2\pi. \quad (4)$$

This assumption is required so that the true acoustic pressure differentials can be approximated by finite differences of the microphones' outputs.

- 2) The desired source signal propagates from the angle $\theta = 0^\circ$ (endfire direction). With this assumption, the signal model (1) becomes

$$\mathbf{y}(\omega) = \mathbf{d}(\omega, 1) X(\omega) + \mathbf{v}(\omega), \quad (5)$$

and, at the endfire, the value of the beamformer's beampattern should always be equal to 1 (or maximal).

With the traditional linear filtering approach, the beamformer output is simply [16]

$$\begin{aligned} Z(\omega) &= \sum_{m=1}^M H_m^*(\omega) Y_m(\omega) \\ &= \mathbf{h}^H(\omega) \mathbf{y}(\omega) \\ &= \mathbf{h}^H(\omega) \mathbf{d}(\omega, 1) X(\omega) + \mathbf{h}^H(\omega) \mathbf{v}(\omega), \end{aligned} \quad (6)$$

where $Z(\omega)$ is the estimate of the desired signal, $X(\omega)$,

$$\mathbf{h}(\omega) \triangleq [H_1(\omega) \quad H_2(\omega) \quad \cdots \quad H_M(\omega)]^T \quad (7)$$

is a complex-valued linear filter applied to the observation signal vector, $\mathbf{y}(\omega)$, and the superscripts $*$ and H denote complex conjugation and conjugate-transpose, respectively. In our context, the distortionless constraint is generally desired, i.e.,

$$\mathbf{h}^H(\omega) \mathbf{d}(\omega, 1) = 1. \quad (8)$$

Without loss of generality, let us choose microphone 1 as the reference. We can then define the input signal-to-noise ratio (SNR) with respect to this reference as

$$\text{iSNR}(\omega) \triangleq \frac{\phi_X(\omega)}{\phi_{V_1}(\omega)}, \quad (9)$$

where $\phi_X(\omega) \triangleq E[|X(\omega)|^2]$ and $\phi_{V_1}(\omega) \triangleq E[|V_1(\omega)|^2]$ are the variances of $X(\omega)$ and $V_1(\omega)$, respectively, with $E[\cdot]$ denoting mathematical expectation.

The output SNR, according to (6), can be written as

$$\begin{aligned} \text{oSNR}[\mathbf{h}(\omega)] &= \phi_X(\omega) \frac{|\mathbf{h}^H(\omega)\mathbf{d}(\omega, 1)|^2}{\mathbf{h}^H(\omega)\mathbf{\Phi}_v(\omega)\mathbf{h}(\omega)} \\ &= \frac{\phi_X(\omega)}{\phi_{V_1}(\omega)} \times \frac{|\mathbf{h}^H(\omega)\mathbf{d}(\omega, 1)|^2}{\mathbf{h}^H(\omega)\mathbf{\Gamma}_v(\omega)\mathbf{h}(\omega)}, \end{aligned} \quad (10)$$

where $\mathbf{\Phi}_v(\omega) \triangleq E[\mathbf{v}(\omega)\mathbf{v}^H(\omega)]$ and $\mathbf{\Gamma}_v(\omega) \triangleq \frac{\mathbf{\Phi}_v(\omega)}{\phi_{V_1}(\omega)}$ are the correlation and pseudo-coherence matrices of $\mathbf{v}(\omega)$, respectively. The definition of the SNR gain is easily derived from (9) and (10), i.e.,

$$\begin{aligned} \mathcal{G}[\mathbf{h}(\omega)] &\triangleq \frac{\text{oSNR}[\mathbf{h}(\omega)]}{\text{iSNR}(\omega)} \\ &= \frac{|\mathbf{h}^H(\omega)\mathbf{d}(\omega, 1)|^2}{\mathbf{h}^H(\omega)\mathbf{\Gamma}_v(\omega)\mathbf{h}(\omega)}. \end{aligned} \quad (11)$$

In practical microphone array systems, microphone sensors always consist of some self noise and there are also mismatch between different sensors, leading to array's imperfections. Generally, array imperfections are modeled as spatially white noise [13], [17]. A commonly used way to evaluate the sensitivity of the array to its imperfections is via the so-called WNG [13], [17], which is defined by taking $\mathbf{\Gamma}_v(\omega) = \mathbf{I}_M$ in (11), where \mathbf{I}_M is the $M \times M$ identity matrix, i.e.,

$$\text{WNG}[\mathbf{h}(\omega)] \triangleq \frac{|\mathbf{h}^H(\omega)\mathbf{d}(\omega, 1)|^2}{\mathbf{h}^H(\omega)\mathbf{h}(\omega)} \leq M. \quad (12)$$

Another important measure, which quantifies how the microphone array performs in the presence of reverberation in room acoustic environments is the DF [18]. Considering the spherically isotropic (diffuse) noise field, the DF is defined as

$$\mathcal{D}[\mathbf{h}(\omega)] \triangleq \frac{|\mathbf{h}^H(\omega)\mathbf{d}(\omega, 1)|^2}{\mathbf{h}^H(\omega)\mathbf{\Gamma}_{0,\pi}(\omega)\mathbf{h}(\omega)}, \quad (13)$$

where the (i, j) th element of the $M \times M$ matrix $\mathbf{\Gamma}_{0,\pi}(\omega)$ is

$$\begin{aligned} [\mathbf{\Gamma}_{0,\pi}(\omega)]_{i,j} &= \frac{\sin[\omega(j-i)\tau_0]}{\omega(j-i)\tau_0} \\ &= \text{sinc}[\omega(j-i)\tau_0], \end{aligned} \quad (14)$$

with $[\mathbf{\Gamma}_{0,\pi}(\omega)]_{m,m} = 1, m = 1, 2, \dots, M$.

From (13), it can be checked that

$$\mathcal{D}[\mathbf{h}(\omega)] \leq \mathbf{d}^H(\omega, 1)\mathbf{\Gamma}_{0,\pi}^{-1}(\omega)\mathbf{d}(\omega, 1). \quad (15)$$

With the beamforming model given in (6), the objective of this paper is to derive a class of filters for the design of any order

DMA beampatterns that have a unique null of maximum multiplicity. To achieve this objective, let us first give the definitions and properties of the DMA beampatterns.

III. BEAMPATTERNS

In this section, we discuss both the theoretical DMA beampattern and the beampattern obtained from the array output with differential beamforming.

A. Theoretical DMA Beampattern

The frequency-independent beampattern of an N th-order theoretical DMA is well known. It can be expressed as [1], [11]

$$\begin{aligned} \mathcal{B}(\mathbf{a}_N, \cos \theta) &= \sum_{n=0}^N a_{N,n} \cos^n \theta \\ &= \mathbf{a}_N^T \mathbf{p}(\cos \theta), \end{aligned} \quad (16)$$

where $a_{N,n}, n = 0, 1, \dots, N$, are real coefficients and

$$\begin{aligned} \mathbf{a}_N &= [a_{N,0} \ a_{N,1} \ \dots \ a_{N,N}]^T, \\ \mathbf{p}(\cos \theta) &= [1 \ \cos \theta \ \dots \ \cos^N \theta]^T. \end{aligned}$$

The different values of the coefficients $a_{N,n}, n = 0, 1, \dots, N$ determine the different beampatterns of the N th-order theoretical DMA. Typically, in the direction of the desired signal, i.e., $\theta = 0^\circ$ by assumption, we would like the beampattern to be equal to 1, i.e., $\mathcal{B}(\mathbf{a}_N, 1) = 1$. Therefore, we have

$$\sum_{n=0}^N a_{N,n} = 1. \quad (17)$$

As a result, we generally choose the first coefficient as

$$a_{N,0} = 1 - \sum_{n=1}^N a_{N,n}. \quad (18)$$

All interesting beampatterns have at least one null in some direction. Since $\cos \theta$ is an even function, so is $\mathcal{B}(\mathbf{a}_N, \cos \theta)$. Therefore, on a polar plot, $\mathcal{B}(\mathbf{a}_N, \cos \theta)$ is symmetric with respect to the axis $0^\circ - 180^\circ$ and any DMA beampattern design can be restricted to this range [6]. It follows from (16) that an N th-order DMA has at most N (distinct) nulls in this range. Let $x = \cos \theta$, we can express (16) as an algebraic polynomial of order N :

$$\begin{aligned} \mathcal{B}(\mathbf{a}_N, x) &= \sum_{n=0}^N a_{N,n} x^n \\ &= \mathbf{a}_N^T \mathbf{p}(x), \end{aligned} \quad (19)$$

where $x \in [-1, 1]$ and

$$\begin{aligned} \mathbf{p}(x) &= [1 \ x \ \dots \ x^N]^T \\ &= [P_0(x) \ P_1(x) \ \dots \ P_N(x)]^T. \end{aligned}$$

A null in the direction θ_0 corresponds to a zero, denoted by $x_0 = \cos \theta_0$, of the polynomial $\mathcal{B}(\mathbf{a}_N, x)$.

Since we are only interested in beampatterns with a unique null of maximum multiplicity, i.e., a multiplicity equal to N , we can write (19) as

$$\mathcal{B}_N(x_0, x) = \frac{1}{(1 - x_0)^N} (x - x_0)^N, \quad (20)$$

with $-1 \leq x_0 < 1$. Two important particular cases of (20) are the dipole ($x_0 = 0$, i.e., a null at 90°) and the cardioid ($x_0 = -1$, i.e., a null at 180°) of order N . It can be checked that [9]

$$\left. \frac{d^i \mathcal{B}_N(x_0, x)}{dx^i} \right|_{x=x_0} = \mathcal{B}_N^{(i)}(x_0, x_0) = 0, \quad (21)$$

where $i = 0, 1, \dots, N-1$ with $\mathcal{B}_N^{(0)}(x_0, x_0) = \mathcal{B}_N(x_0, x_0)$. As a result, the i th derivative of $\mathcal{B}(\mathbf{a}_N, x)$ with respect to x at x_0 is

$$\mathcal{B}^{(i)}(\mathbf{a}_N, x_0) = \sum_{n=0}^N a_{N,n} P_n^{(i)}(x_0) = 0, \quad i = 0, 1, \dots, N-1, \quad (22)$$

with $P_n^{(0)}(x_0) = P_n(x_0)$. Using the fact that

$$\mathcal{B}(\mathbf{a}_N, 1) = \sum_{n=0}^N a_{N,n} P_n(1) = 1, \quad (23)$$

we obtain a linear system of $N+1$ equations:

$$\mathbf{P}(x_0) \mathbf{a}_N = \mathbf{i}, \quad (24)$$

where

$$\mathbf{P}(x_0) = \begin{bmatrix} P_0(1) & P_1(1) & \cdots & P_N(1) \\ P_0^{(0)}(x_0) & P_1^{(0)}(x_0) & \cdots & P_N^{(0)}(x_0) \\ \vdots & \vdots & \ddots & \vdots \\ P_0^{(N-1)}(x_0) & P_1^{(N-1)}(x_0) & \cdots & P_N^{(N-1)}(x_0) \end{bmatrix} \quad (25)$$

and

$$\mathbf{i} = [1 \quad 0 \quad \cdots \quad 0]^T \quad (26)$$

is a vector of length $N+1$. Therefore, the coefficient vector of the beampatterns with a unique null of multiplicity N is

$$\mathbf{a}_N(x_0) = \mathbf{P}^{-1}(x_0) \mathbf{i}. \quad (27)$$

And the corresponding beampattern is

$$\mathcal{B}_N(x_0, x) = \mathbf{i}^T \mathbf{P}^{-1}(x_0) \mathbf{p}(x). \quad (28)$$

B. Beampattern of a DMA Beamformer

The beampattern corresponding to the beamformer $\mathbf{h}(\omega)$ is mathematically defined as

$$\begin{aligned} \mathcal{B}[\mathbf{h}(\omega), x] &\triangleq \mathbf{d}^H(\omega, x) \mathbf{h}(\omega) \\ &= \sum_{m=1}^M H_m(\omega) e^{j(m-1)\omega\tau_0 x}. \end{aligned} \quad (29)$$

The objective of differential beamforming or DMA beampattern design is to find an appropriate filter, $\mathbf{h}(\omega)$, so that $\mathcal{B}[\mathbf{h}(\omega), x]$ is the same (or approximately the same) as the theoretical beampattern given in (28).

IV. APPROACH I: TRADITIONAL DMAS

In the way traditional DMAs are designed, we always take the number of microphones equal to the order plus one, i.e., $M = N + 1$.

A. Derivation

Let us denote by x_0 the zero of multiplicity $N = M - 1$ of $\mathcal{B}[\mathbf{h}(\omega), x]$. Applying the property that the i th derivative, with $i = 0, 1, \dots, M - 2$, of the beampattern with respect to x is equal to 0 at x_0 , i.e.,

$$\left. \frac{d^i \mathcal{B}[\mathbf{h}(\omega), x]}{dx^i} \right|_{x=x_0} = \mathcal{B}^{(i)}[\mathbf{h}(\omega), x_0] = 0, \quad (30)$$

with $\mathcal{B}^{(0)}[\mathbf{h}(\omega), x_0] = \mathcal{B}[\mathbf{h}(\omega), x_0]$, we easily get $\forall i = 0, 1, \dots, M - 2$,

$$\mathcal{B}^{(i)}[\mathbf{h}(\omega), x_0] = (j\omega\tau_0)^i [\boldsymbol{\Sigma}^i \mathbf{d}(\omega, x_0)]^H \mathbf{h}(\omega), \quad (31)$$

where

$$\boldsymbol{\Sigma} = \text{diag}(0, 1, \dots, M-1) \quad (32)$$

is a diagonal matrix of size $M \times M$. Combining the distortionless constraint, i.e.,

$$\mathcal{B}[\mathbf{h}(\omega), 1] = \mathbf{d}^H(\omega, 1) \mathbf{h}(\omega) = 1, \quad (33)$$

with the $M - 1$ equations from (31), we obtain a linear system of M equations with M unknowns [9]:

$$\mathbf{D}(\omega, x_0) \mathbf{h}(\omega) = \mathbf{i}, \quad (34)$$

where

$$\mathbf{D}(\omega, x_0) = \begin{bmatrix} \mathbf{d}^H(\omega, 1) \\ [\boldsymbol{\Sigma}^0 \mathbf{d}(\omega, x_0)]^H \\ [\boldsymbol{\Sigma}^1 \mathbf{d}(\omega, x_0)]^H \\ \vdots \\ [\boldsymbol{\Sigma}^{M-2} \mathbf{d}(\omega, x_0)]^H \end{bmatrix} \quad (35)$$

and \mathbf{i} is the first column of \mathbf{I}_M . Consequently, the optimal filter with this approach is

$$\mathbf{h}_C(\omega, x_0) = \mathbf{D}^{-1}(\omega, x_0) \mathbf{i}. \quad (36)$$

B. Evaluation

Figs. 1 and 2 plot the beampatterns and SNR gains of $\mathbf{h}_C(\omega, x_0)$ with $M = 4$, $N = 3$, and $\delta = 1$ cm. Two values of θ_0 are considered in this evaluation, i.e., 90° and 180° .

According to [10], the beampattern of this beamformer can be well approximated by (20) if the assumption (4) holds. As a result, the beampattern is almost frequency invariant (see Fig. 1), so is the DF [see Fig. 2(a)].

As shown in Appendix A, the WNG of this filter is given by

$$\mathcal{W}[\mathbf{h}_C(\omega, x_0)] = \frac{2^N}{C_{2N}^N} \{1 - \cos[\omega\tau_0(1-x_0)]\}^N, \quad (37)$$

where C_{2N}^N is defined in (61).

Considering the assumption given in (4), we have $\cos[\omega\tau_0(1-x_0)] \approx 1 - \frac{1}{2}[\omega\tau_0(1-x_0)]^2$. As a result, (37) can be approximately expressed as

$$\mathcal{W}[\mathbf{h}_C(\omega, x_0)] \approx \frac{1}{C_{2N}^N} (\omega\tau_0)^{2N} (1-x_0)^{2N}. \quad (38)$$

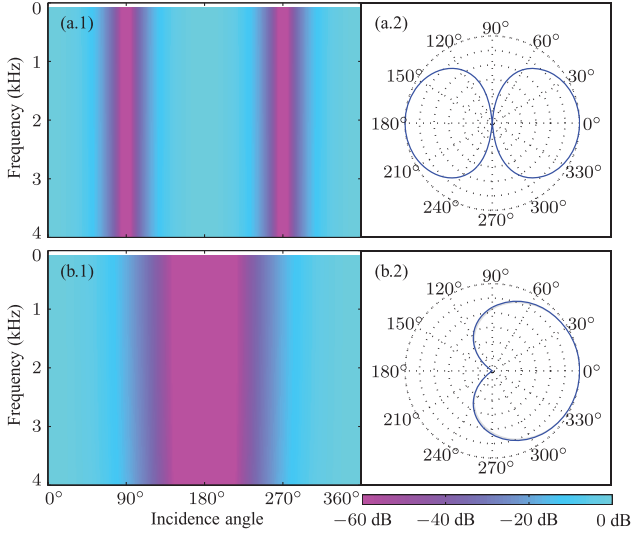


Fig. 1. Beampatterns of $\mathbf{h}_C(\omega, x_0)$ with different null positions. [(a.1), (a.2): $\theta_0 = 90^\circ$; (b.1), (b.2): $\theta_0 = 180^\circ$]. $M = 4$, $N = 3$, $\delta = 1$ cm, and (a.2) and (b.2) are plotted at 4 kHz.

Clearly, the WNG goes to zero as the frequency goes to zero [see Fig. 2(b)], indicating that the uncorrelated noise is dramatically amplified at low frequencies.

Since the WNG is a monotonically decreasing function with respect to x_0 , it can be improved by simply making the null approach 180° ; for example, the difference in WNG between the cardioid and dipole is $6N$ dB.

V. APPROACH II: MAXIMIZATION OF THE WNG

In this and the subsequent approaches, we consider the more interesting case where the number of microphones is greater than the DMA order plus one, i.e., $M > N + 1$. As a consequence, we can make a better compromise among the WNG, the DF, and the frequency-invariance of the beampatterns.

A. Derivation

Equation (34) can be extended to

$$\mathbf{D}'(\omega, x_0)\mathbf{h}(\omega) = \mathbf{i}, \quad (39)$$

where

$$\mathbf{D}'(\omega, x_0) = \begin{bmatrix} \mathbf{d}^H(\omega, 1) \\ [\boldsymbol{\Sigma}^0 \mathbf{d}(\omega, x_0)]^H \\ [\boldsymbol{\Sigma}^1 \mathbf{d}(\omega, x_0)]^H \\ \vdots \\ [\boldsymbol{\Sigma}^{N-1} \mathbf{d}(\omega, x_0)]^H \end{bmatrix} \quad (40)$$

is now an $(N + 1) \times M$ matrix and \mathbf{i} is the first column of the $(N + 1) \times (N + 1)$ identity matrix \mathbf{I}_{N+1} .

In order to deal with the white noise amplification problem, we propose to maximize the WNG given the constraint (39), which can be translated into the following optimization problem:

$$\min_{\mathbf{h}(\omega)} \mathbf{h}^H(\omega)\mathbf{h}(\omega) \text{ subject to } \mathbf{D}'(\omega, x_0)\mathbf{h}(\omega) = \mathbf{i}. \quad (41)$$

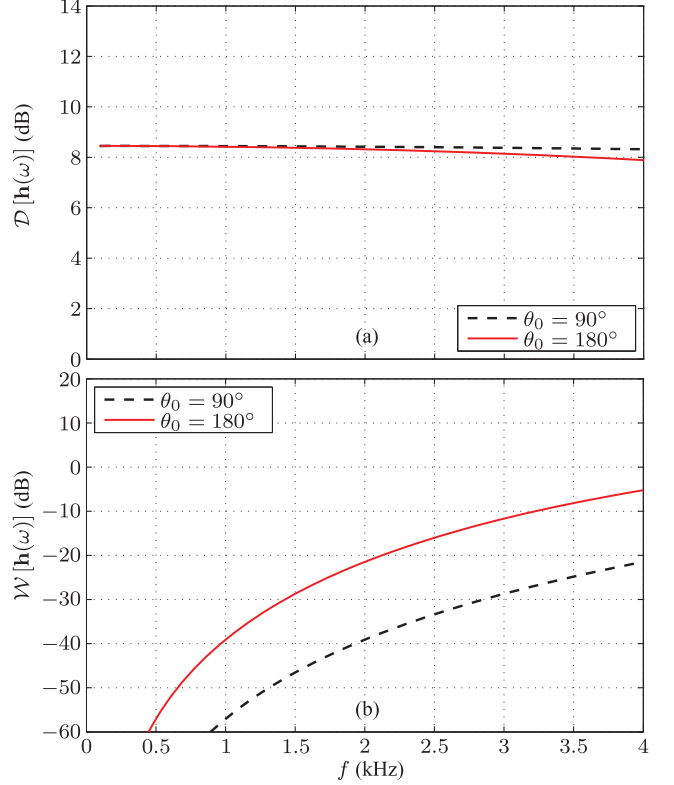


Fig. 2. SNR gains of $\mathbf{h}_C(\omega, x_0)$ as a function of frequency with different null positions: (a) DF and (b) WNG. $M = 4$, $N = 3$, and $\delta = 1$ cm.

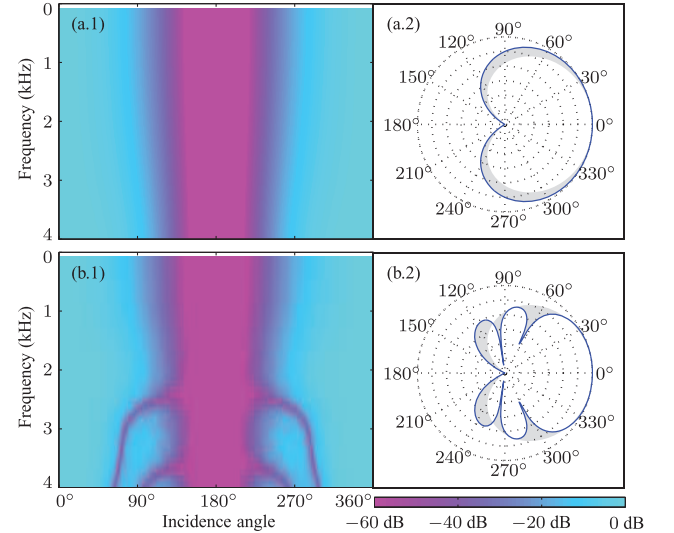


Fig. 3. Beampatterns of $\mathbf{h}_{WN}(\omega, x_0)$ with different numbers of sensors [(a.1), (a.2): $M = 8$; and (b.1), (b.2): $M = 16$]. $\theta_0 = 180^\circ$, $N = 3$, $\delta = 1$ cm, and (a.2) and (b.2) are plotted at 4 kHz. The gray region is the difference between the obtained and desired beampatterns.

It follows then that the optimal beamformer is

$$\mathbf{h}_{WN}(\omega, x_0) = \mathbf{D}'^H(\omega, x_0) \left[\mathbf{D}'(\omega, x_0) \mathbf{D}'^H(\omega, x_0) \right]^{-1} \mathbf{i}, \quad (42)$$

which is also the minimum-norm solution of (39).

B. Evaluation

Figs. 3 and 4 plot the beampatterns and SNR gains of $\mathbf{h}_{WN}(\omega, x_0)$ with $N = 3$, $\delta = 1$ cm, and $\theta_0 = 180^\circ$. Three values of M are considered in this evaluation, i.e., 4, 8, and 16.

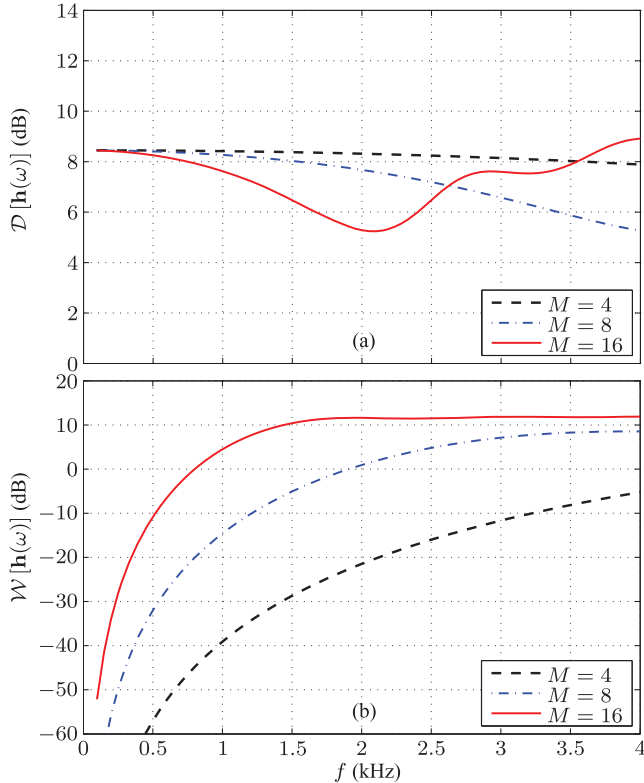


Fig. 4. SNR gains of $\mathbf{h}_{\text{WN}}(\omega, x_0)$ with different numbers of sensors: (a) DF and (b) WNG. $\theta_0 = 180^\circ$, $N = 3$, and $\delta = 1$ cm.

As shown in Appendix 10, the WNG improvement of this filter can be deduced as

$$\mathcal{R}_W(\omega\tau_0, x_0) \triangleq \frac{\mathcal{W}[\mathbf{h}_{\text{WN}}(\omega, x_0)]}{\mathcal{W}[\mathbf{h}_{\text{C}}(\omega, x_0)]} \quad (43)$$

$$= C_{2N}^N \mathbf{d}''^H(\omega, x_0) \mathbf{\Xi}^{-1} \mathbf{d}''(\omega, x_0), \quad (44)$$

where the vector $\mathbf{d}''(\omega, x_0)$ and the constant matrix $\mathbf{\Xi}$ are defined in (74) and (77), respectively. Clearly, we have

$$\lim_{\omega\tau_0 \rightarrow 0} \mathcal{R}_W(\omega\tau_0, x_0) = C_{2N}^N \boldsymbol{\eta}^T \mathbf{\Xi}^{-1} \boldsymbol{\eta}, \quad (45)$$

where $\boldsymbol{\eta} = [1 \ 1 \ \dots \ 1]^T$ is a constant vector of length $M - N$; therefore, at low frequencies, the WNG improvement rarely depends on the null direction. According to (38), (43), and (45), one can conclude that, in terms of robustness, the cardioid is the best.

While it improves the WNG [see Fig. 4(b)], the minimum-norm approach may deform the beampatterns (see Fig. 3) and sacrifices the DFs [see Fig. 4(a)], particularly at high frequencies.

VI. APPROACH III: MINIMIZATION OF THE DIFFUSE NOISE

A. Derivation

The most straightforward way to improve the DF of a DMA is by maximizing the DF subject to the constraint (39), which can be written into the following problem:

$$\min_{\mathbf{h}(\omega)} \mathbf{h}^H(\omega) \boldsymbol{\Gamma}_{0,\pi}(\omega) \mathbf{h}(\omega) \text{ subject to } \mathbf{D}'(\omega, x_0) \mathbf{h}(\omega) = \mathbf{i}. \quad (46)$$

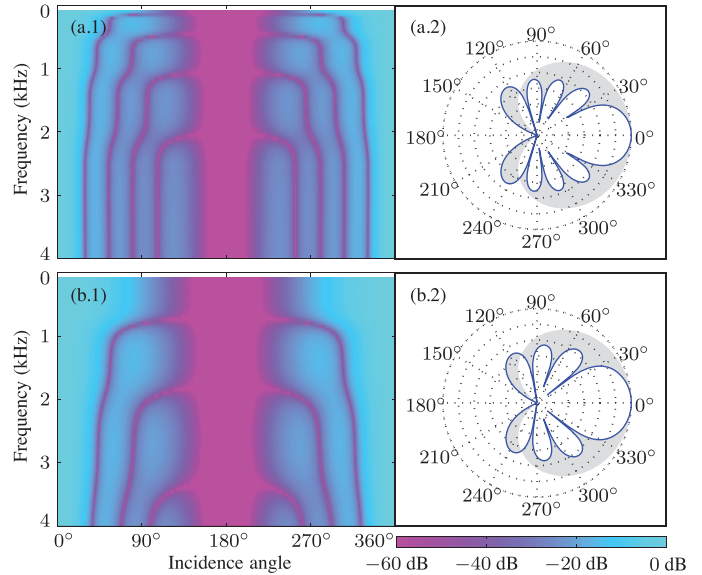


Fig. 5. Beampatterns of $\mathbf{h}_{\text{DN},\epsilon}(\omega, x_0)$ with different values of the regularization parameter [(a.1), (a.2): $\epsilon = 10^{-12}$; and (b.1), (b.2): $\epsilon = 10^{-6}$]. $\theta_0 = 180^\circ$, $M = 8$, $N = 3$, $\delta = 1$ cm, and (a.2) and (b.2) are plotted at 4 kHz. The gray region is the difference between the obtained and desired beampatterns.

As a result, the optimal filter is

$$\begin{aligned} \mathbf{h}_{\text{DN}}(\omega, x_0) &= \boldsymbol{\Gamma}_{0,\pi}^{-1}(\omega) \mathbf{D}'^H(\omega, x_0) \\ &\times \left[\mathbf{D}'(\omega, x_0) \boldsymbol{\Gamma}_{0,\pi}^{-1}(\omega) \mathbf{D}'^H(\omega, x_0) \right]^{-1} \mathbf{i}. \end{aligned} \quad (47)$$

It is well known that $\boldsymbol{\Gamma}_{0,\pi}(\omega)$ is very ill-conditioned at low frequencies, see the Fig. 2 in [19] as an example; as a result, the WNG of this filter is usually much worse than that of the traditional approach. In order to better deal with this problem, we suggest the following regularized beamformer:

$$\begin{aligned} \mathbf{h}_{\text{DN},\epsilon}(\omega, x_0) &= \boldsymbol{\Gamma}_\epsilon^{-1}(\omega) \mathbf{D}'^H(\omega, x_0) \\ &\times \left[\mathbf{D}'(\omega, x_0) \boldsymbol{\Gamma}_\epsilon^{-1}(\omega) \mathbf{D}'^H(\omega, x_0) \right]^{-1} \mathbf{i}, \end{aligned} \quad (48)$$

where

$$\boldsymbol{\Gamma}_\epsilon(\omega) = \boldsymbol{\Gamma}_{0,\pi}(\omega) + \epsilon \mathbf{I}_M, \quad (49)$$

with $\epsilon \geq 0$ being the regularization parameter. It is clear that $\mathbf{h}_{\text{DN},0}(\omega, x_0) = \mathbf{h}_{\text{DN}}(\omega, x_0)$ and $\mathbf{h}_{\text{DN},\infty}(\omega, x_0) = \mathbf{h}_{\text{WN}}(\omega, x_0)$.

B. Evaluation

Fig. 5 plots the beampatterns of $\mathbf{h}_{\text{DN},\epsilon}(\omega, x_0)$ with $M = 8$, $N = 3$, $\theta_0 = 180^\circ$, and $\delta = 1$ cm. Two values of ϵ are considered in this evaluation, i.e., $\epsilon = 10^{-12}$ and $\epsilon = 10^{-6}$.

It is seen from Fig. 5 that with the $\mathbf{h}_{\text{DN},\epsilon}(\omega, x_0)$ beamformer, extra nulls appear in the beampattern besides those at θ_0 , which is undesirable. The underlying reason may be explained as follows. The diffuse noise has a uniform distribution of energy over the entire space. To minimize the variance of the diffuse noise, thereby maximizing the DF, the beamformer needs to place as

many nulls as possible (which depends on the number of sensors) and as uniform as possible in all directions under the given mainlobe and null constraints. The maximum number of extra nulls is $M - N - 1$.

VII. APPROACH IV: WEIGHTED-NORM DESIGN

A. Derivation

Let $w(x)$ be a weight function defined on the interval $[-1, 1]$ with $w(x) > 0 \forall x \in [-1, 1]$, so that

$$\int_{-1}^1 w(x) dx > 0. \quad (50)$$

We define the square norm of $\mathcal{B}[\mathbf{h}(\omega), x]$ with respect to the weight function $w(x)$ as

$$\begin{aligned} \|\mathcal{B}[\mathbf{h}(\omega), x]\|_w^2 &= \mathcal{N}_w \int_{-1}^1 w(x) |\mathcal{B}[\mathbf{h}(\omega), x]|^2 dx \\ &= \mathbf{h}^H(\omega) \mathbf{\Gamma}_w(\omega) \mathbf{h}(\omega), \end{aligned} \quad (51)$$

where

$$\mathbf{\Gamma}_w(\omega) = \mathcal{N}_w \int_{-1}^1 w(x) \mathbf{d}(\omega, x) \mathbf{d}^H(\omega, x) dx, \quad (52)$$

which can be viewed as the pseudo-coherence matrix of the spatial noise with the distribution $w(x)$, and

$$\mathcal{N}_w = \frac{1}{\int_{-1}^1 w(x) dx} \quad (53)$$

is a normalization factor.

By minimizing $\|\mathcal{B}[\mathbf{h}(\omega), x]\|_w^2$ subject to (39), i.e.,

$$\min_{\mathbf{h}(\omega)} \mathbf{h}^H(\omega) \mathbf{\Gamma}_w(\omega) \mathbf{h}(\omega) \text{ subject to } \mathbf{D}'(\omega, x_0) \mathbf{h}(\omega) = \mathbf{i}, \quad (54)$$

we deduce the solution:

$$\begin{aligned} \mathbf{h}_w(\omega, x_0) &= \mathbf{\Gamma}_w^{-1}(\omega) \mathbf{D}'^H(\omega, x_0) \\ &\times \left[\mathbf{D}'(\omega, x_0) \mathbf{\Gamma}_w^{-1}(\omega) \mathbf{D}'^H(\omega, x_0) \right]^{-1} \mathbf{i}. \end{aligned} \quad (55)$$

The beampattern degradation of this filter can be well controlled by properly choosing the weight function $w(x)$, which cannot be done with the filter $\mathbf{h}_{\text{DN}}(\omega, x_0)$.

To handle the ill-conditioning issue of $\mathbf{\Gamma}_w(\omega)$, we suggest a more robust version:

$$\begin{aligned} \mathbf{h}_{w,\epsilon}(\omega, x_0) &= \mathbf{\Gamma}_{w,\epsilon}^{-1}(\omega) \mathbf{D}'^H(\omega, x_0) \\ &\times \left[\mathbf{D}'(\omega, x_0) \mathbf{\Gamma}_{w,\epsilon}^{-1}(\omega) \mathbf{D}'^H(\omega, x_0) \right]^{-1} \mathbf{i}, \end{aligned} \quad (56)$$

where

$$\mathbf{\Gamma}_{w,\epsilon}(\omega) = \mathbf{\Gamma}_w(\omega) + \epsilon \mathbf{I}_M. \quad (57)$$

For $w(x) = 1$, we have $\mathbf{h}_w(\omega, x_0) = \mathbf{h}_{\text{DN}}(\omega, x_0)$ and $\mathbf{h}_{w,\epsilon}(\omega, x_0) = \mathbf{h}_{\text{DN},\epsilon}(\omega, x_0)$.

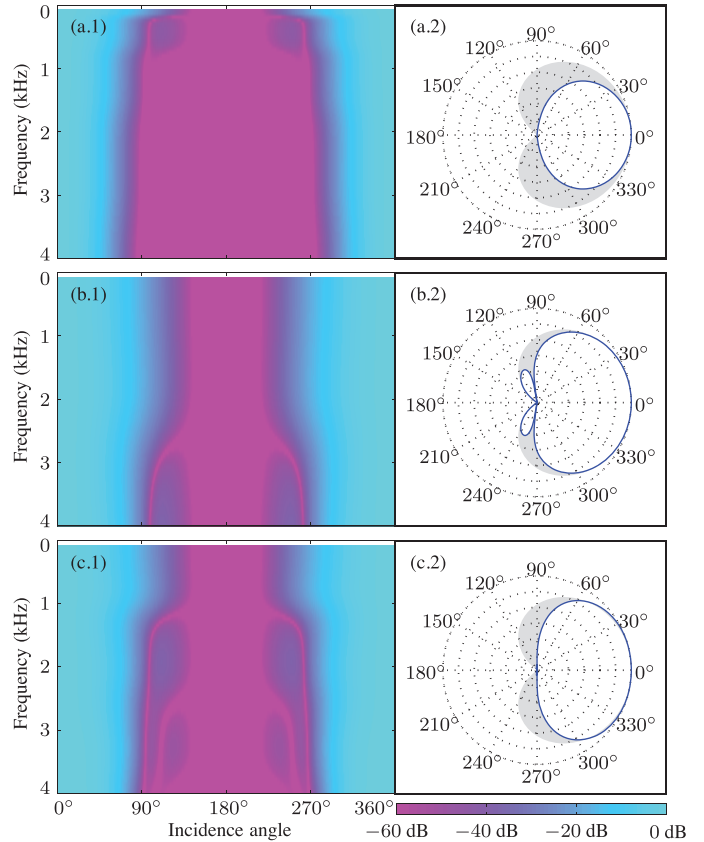


Fig. 6. Beampatterns of $\mathbf{h}_{w,\epsilon}(\omega, x_0)$ with different numbers of sensors and values of the regularization parameter [(a.1), (a.2): $M = 8$ and $\epsilon = 10^{-12}$; (b.1), (b.2): $M = 8$ and $\epsilon = 10^{-3}$; and (c.1), (c.2): $M = 16$ and $\epsilon = 10^{-3}$]. $\theta_0 = 180^\circ$, $N = 3$, $\delta = 1$ cm, and (a.2), (b.2), and (c.2) are plotted at 4 kHz. The gray region is the difference between the obtained and desired beampatterns.

B. Evaluation

The weight function $w(x)$ can be viewed as the spatial distribution of the noise. It influences the nulls' distribution of the obtained beampattern. In this simulation, we choose

$$w(x) = \begin{cases} 1, & -1 \leq x < 0 \\ 0, & 0 \leq x \leq 1 \end{cases}, \quad (58)$$

which means that the noise is uniformly distributed in the region of $[90^\circ, 270^\circ]$.

The beampatterns and SNR gains are shown in Figs. 6 and 7, respectively. The following observations are in order.

- In the case of $\epsilon = 10^{-12}$, the beampattern is almost frequency independent [see Fig. 6(a.1)]. The mainlobe in this case is much narrower than that with the conventional method as seen in Fig. 6(a.2) and, as a result, the DF is higher than the expected value [see the dash black line in Fig. 7(a)]; however, the WNG is dramatically low [see the dash black line in Fig. 7(b)].
- By increasing the value of the regularization parameter, ϵ , the WNG can be greatly improved [see the dash-dot blue line in Fig. 7(b)]. At the same time, the beampattern and the DF are almost frequency independent [see Fig. 6(b.1) and the dash-dot blue line in Fig. 7(a)].
- By increasing the number of sensors, we can further improve the WNG [see the solid red line in Fig. 7(b)].

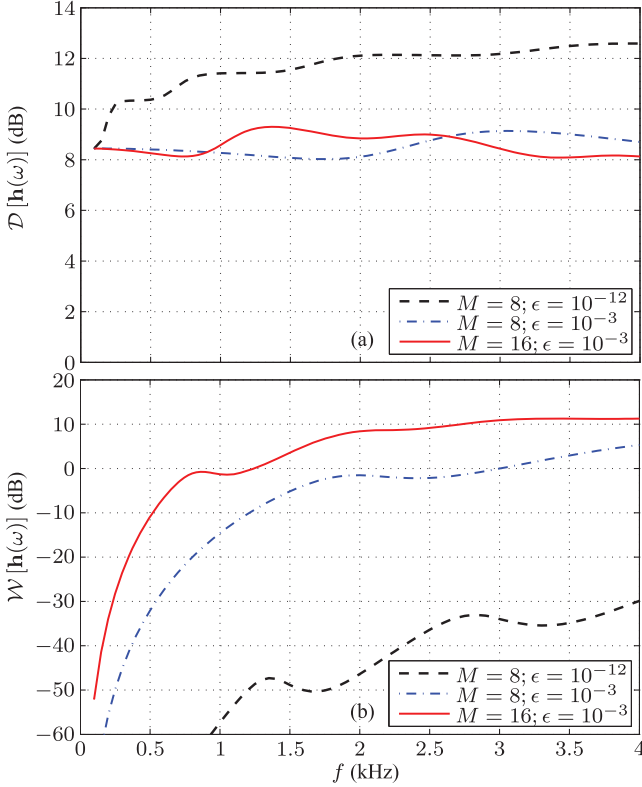


Fig. 7. SNR gains of $\mathbf{h}_{w,\epsilon}(\omega, x_0)$ with different numbers of sensors and values of the regularization parameter: (a) DF and (b) WNG. $\theta_0 = 180^\circ$, $N = 3$, and $\delta = 1$ cm.

without affecting much the DF and the beampattern [see Fig. 6(c.1) and the solid red line in Fig. 7(a)].

In practice, we may choose different regularization parameters at different frequencies. Particularly, we can use a large value of ϵ at low frequencies for a better WNG improvement while use a small value of ϵ at high frequencies where the WNG is rarely a problem but the beampattern may easily get deformed.

VIII. CONCLUSIONS

In this paper, we showed how to design the particular class of DMA beampatterns that have a unique null of maximum multiplicity. We proved, among other things, that the cardioid is the best in terms of robustness to spatially white noise. Considering the fact that DMAs may suffer significantly from white noise amplification, we developed a weighted-norm DMA design approach that can control the compromise among the beampattern, the DF, and the WNG.

APPENDIX A PROOF OF (37)

According to [10], the spatial \mathcal{Z} transform of the beamformer with multiple nulls in the same direction can be written as

$$\begin{aligned} \mathcal{H}(\mathcal{Z}) &\triangleq \sum_{n=0}^N H_{n+1}(\omega) \mathcal{Z}^{-n} \\ &= \frac{1}{\zeta(\omega, x_0)} (e^{j\omega\tau_0 x_0} - \mathcal{Z}^{-1})^N \end{aligned}$$

$$\begin{aligned} &= \frac{1}{\zeta(\omega, x_0)} \sum_{n=0}^N (-1)^n C_N^n e^{j(N-n)\omega\tau_0 x_0} \mathcal{Z}^{-n} \\ &= \frac{e^{jN\omega\tau_0 x_0}}{\zeta(\omega, x_0)} \sum_{n=0}^N (-1)^n C_N^n e^{-jn\omega\tau_0 x_0} \mathcal{Z}^{-n}, \end{aligned} \quad (59)$$

where $\mathcal{Z}^{-1} = e^{j\omega\tau_0}$,

$$\zeta(\omega, x_0) \triangleq (e^{j\omega\tau_0 x_0} - e^{j\omega\tau_0})^N \quad (60)$$

is the normalization factor to satisfy the distortionless constraint in (8), and

$$C_N^n \triangleq \frac{N!}{n!(N-n)!} \quad (61)$$

is the binomial coefficient. Since the weight of the m th ($m = 1, 2, \dots, N+1$) sensor is the coefficient of $\mathcal{Z}^{-(m-1)}$, we deduce that the traditional beamformer can be rewritten as

$$\mathbf{h}_C(\omega, x_0) = \frac{e^{jN\omega\tau_0 x_0}}{\zeta(\omega, x_0)} \begin{bmatrix} 1 \\ -C_N^1 e^{-j\omega\tau_0 x_0} \\ C_N^2 e^{-j2\omega\tau_0 x_0} \\ \vdots \\ (-1)^N C_N^N e^{-jN\omega\tau_0 x_0} \end{bmatrix}. \quad (62)$$

Substituting (62) into (12), we finally find the WNG of the traditional beamformer:

$$\begin{aligned} \mathcal{W}[\mathbf{h}_C(\omega, x_0)] &= \frac{|\zeta(\omega, x_0)|^2}{\sum_{n=0}^N (C_N^n)^2} \\ &= \frac{2^N}{C_{2N}^N} \{1 - \cos[\omega\tau_0(1-x_0)]\}^N. \end{aligned} \quad (63)$$

APPENDIX B PROOF OF (44)

In [10], we obtained an equivalent form of the robust (minimum-norm) beamforming filter with the two-stage framework:

$$\mathbf{h}_{\text{WN}}(\omega, x_0) = \frac{\mathbf{H}(\omega, x_0) [\mathbf{H}^H(\omega, x_0) \mathbf{H}(\omega, x_0)]^{-1} \mathbf{d}'(\omega)}{\mathbf{d}'(\omega) [\mathbf{H}^H(\omega, x_0) \mathbf{H}(\omega, x_0)]^{-1} \mathbf{d}'(\omega)}, \quad (64)$$

where the (i, j) th element of $\mathbf{H}(\omega, x_0)$ is

$$[\mathbf{H}(\omega, x_0)]_{i,j} = \begin{cases} [\mathbf{h}_C(\omega, x_0)]_{i-j+1}, & j \leq i \leq j+N \\ 0, & \text{else} \end{cases} \quad (65)$$

and the vector $\mathbf{d}'(\omega)$ is defined as

$$\mathbf{d}'(\omega) = [1 \quad e^{-j\omega\tau_0} \quad \dots \quad e^{-j(M-N-1)\omega\tau_0}]^T. \quad (66)$$

Substituting (64) into (12), we deduce the WNG of the robust filter:

$$\mathcal{W}[\mathbf{h}_{\text{WN}}(\omega, x_0)] = \mathbf{d}'^H(\omega) \mathbf{\Psi}^{-1}(\omega, x_0) \mathbf{d}'(\omega), \quad (67)$$

where

$$\mathbf{\Psi}(\omega, x_0) = \mathbf{H}^H(\omega, x_0) \mathbf{H}(\omega, x_0). \quad (68)$$

Substituting (65) into (68), we get the (i, j) th element of $\Psi(\omega, x_0)$:

$$\begin{aligned} [\Psi(\omega, x_0)]_{i,j} &= \sum_{\ell=\ell_{\min}}^{\ell_{\max}} [\mathbf{H}^H(\omega, x_0)]_{i,\ell} [\mathbf{H}(\omega, x_0)]_{\ell,j} \\ &= \sum_{\ell=\ell_{\min}}^{\ell_{\max}} [\mathbf{H}(\omega, x_0)]_{\ell,i}^* [\mathbf{H}(\omega, x_0)]_{\ell,j} \\ &= \sum_{\ell=\ell_{\min}}^{\ell_{\max}} [\mathbf{h}_C(\omega, x_0)]_{\ell-i+1}^* [\mathbf{h}_C(\omega, x_0)]_{\ell-j+1}, \end{aligned} \quad (69)$$

where

$$\ell_{\min} = \max\{i, j\}, \quad (70)$$

$$\ell_{\max} = \min\{N + i, N + j\}. \quad (71)$$

Substituting (62) into (69), we deduce that $\forall |i - j| \leq N$,

$$\begin{aligned} [\Psi(\omega, x_0)]_{i,j} &= \frac{e^{j(i-j)\omega\tau_0 x_0}}{|\zeta(\omega, x_0)|^2} \sum_{\ell=\ell_{\min}}^{\ell_{\max}} (-1)^{2\ell-i-j} C_N^{\ell-i} C_N^{\ell-j} \\ &= \frac{e^{j(i-j)\omega\tau_0 x_0}}{|\zeta(\omega, x_0)|^2} (-1)^{i-j} \sum_{\ell=0}^{N-(i-j)} C_N^{\ell} C_N^{\ell+(i-j)} \\ &= \frac{1}{|\zeta(\omega, x_0)|^2} (-1)^{i-j} C_{2N}^{N-(i-j)} e^{j(i-j)\omega\tau_0 x_0}, \end{aligned} \quad (72)$$

where $\zeta(\omega, x_0)$ is defined in (60). Therefore, we can rewrite $\Psi(\omega, x_0)$ as

$$\Psi(\omega, x_0) = \frac{1}{|\zeta(\omega, x_0)|^2} \mathbf{\Lambda}(\omega, x_0) \mathbf{\Xi} \mathbf{\Lambda}^H(\omega, x_0), \quad (73)$$

where the (i, j) th element of $\mathbf{\Xi}$ is

$$[\mathbf{\Xi}]_{i,j} = \begin{cases} (-1)^{i-j} C_{2N}^{N-(i-j)}, & |i - j| \leq N \\ 0, & \text{else} \end{cases} \quad (74)$$

and

$$\mathbf{\Lambda}(\omega, x_0) = \text{diag} [1, e^{j\omega\tau_0 x_0}, \dots, e^{j(M-N-1)\omega\tau_0 x_0}] \quad (75)$$

is a diagonal matrix. Substituting (73) into (67) gives the WNG of the robust filter:

$$\mathcal{W}[\mathbf{h}_{\text{WN}}(\omega, x_0)] = |\zeta(\omega, x_0)|^2 \mathbf{d}''^H(\omega, x_0) \mathbf{\Xi}^{-1} \mathbf{d}''(\omega, x_0), \quad (76)$$

where

$$\mathbf{d}''(\omega, x_0) = \begin{bmatrix} 1 \\ e^{-j\omega\tau_0(1-x_0)} \\ \vdots \\ e^{-j(M-N-1)\omega\tau_0(1-x_0)} \end{bmatrix}. \quad (77)$$

Combining (63) with (76) gives the WNG improvement of the robust filter:

$$\mathcal{R}_W(\omega\tau_0, x_0) = C_{2N}^N \mathbf{d}''^H(\omega, x_0) \mathbf{\Xi}^{-1} \mathbf{d}''(\omega, x_0). \quad (78)$$

REFERENCES

- [1] J. Benesty and J. Chen, *Study and Design of Differential Microphone Arrays*. Berlin, Germany: Springer-Verlag, 2012.
- [2] G. W. Elko and A.-T. N. Pong, "A simple adaptive first-order differential microphone," in *Proc. IEEE Workshop Appl. Signal Process. Audio Acoust. (WASPAA)*, 1995, pp. 169–172.
- [3] M. Buck, "Aspects of first-order differential microphone arrays in the presence of sensor imperfections," *Eur. Trans. Telecommun.*, vol. 13, pp. 115–122, Mar.–Apr. 2002.
- [4] G. W. Elko and J. Meyer, "Microphone arrays," in *Springer Handbook of Speech Processing*, J. Benesty, M. M. Sondhi, and Y. Huang, Eds. Berlin, Germany: Springer-Verlag, 2008, ch. 50, pp. 1021–1041.
- [5] T. D. Abhayapala and A. Gupta, "Higher order differential-integral microphone arrays," *J. Acoust. Soc. Amer.*, vol. 127, pp. EL227–EL233, May 2010.
- [6] E. De Sena, H. Hacıhabiboglu, and Z. Cvetkovic, "On the design and implementation of higher-order differential microphones," *IEEE Trans. Audio, Speech, Lang. Process.*, vol. 20, no. 1, pp. 162–174, Jan. 2012.
- [7] J. Benesty, M. Souden, and Y. Huang, "A perspective on differential microphone arrays in the context of noise reduction," *IEEE Trans. Audio, Speech, Lang. Process.*, vol. 20, no. 2, pp. 699–704, Feb. 2012.
- [8] J. Chen and J. Benesty, "A general approach to the design and implementation of linear differential microphone arrays," in *Proc. Asia-Pacific Signal Inf. Process. Assoc. Annu. Summit Conf. (APSIPA)*, 2013.
- [9] J. Chen, J. Benesty, and C. Pan, "On the design and implementation of linear differential microphone arrays," *J. Acoust. Soc. Amer.*, vol. 136, pp. 3097–3113, Dec. 2014.
- [10] C. Pan, J. Chen, and J. Benesty, "Theoretical analysis of differential microphone array beamforming and an improved solution," *IEEE/ACM Trans. Audio, Speech, Lang. Process.*, vol. 23, no. 11, pp. 2093–2105, Nov. 2015.
- [11] G. W. Elko, "Superdirectional microphone arrays," in *Acoustic Signal Processing for Telecommunication*, S. L. Gay and J. Benesty, Eds. Boston, MA, USA: Kluwer, 2000, ch. 10, pp. 181–237.
- [12] H. Cox, R. M. Zeskind, and T. Kooij, "Practical supergain," *IEEE Trans. Acoust., Speech, Signal Process.*, vol. ASSP-34, no. 3, pp. 393–398, Jun. 1986.
- [13] S. Yan and Y. Ma, "Robust supergain beamforming for circular array via second-order cone programming," *Appl. Acoust.*, vol. 66, no. 9, pp. 1018–1032, Sep. 2005.
- [14] L. Zhao, J. Benesty, and J. Chen, "Design of robust differential microphone arrays," *IEEE/ACM Trans. Audio, Speech, Lang. Process.*, vol. 22, no. 10, pp. 1455–1466, Oct. 2014.
- [15] C. Pan, J. Benesty, and J. Chen, "Design of robust differential microphone arrays with orthogonal polynomials," *J. Acoust. Soc. Amer.*, vol. 138, no. 2, pp. 1079–1089, Aug. 2015.
- [16] J. Benesty, J. Chen, and Y. Huang, *Microphone Array Signal Processing*. Berlin, Germany: Springer-Verlag, 2008.
- [17] E. N. Gilbert and S. P. Morgan, "Optimum design of directive antenna arrays subject to random variations," *Bell Syst. Tech. J.*, vol. 34, no. 3, pp. 637–663, May 1955.
- [18] R. N. Marshall and W. R. Harry, "A new microphone providing uniform directivity over an extended frequency range," *J. Acoust. Soc. Amer.*, vol. 12, no. 4, pp. 481–498, Apr. 1941.
- [19] C. Pan, J. Chen, and J. Benesty, "A multistage minimum variance distortionless response beamformer for noise reduction," *J. Acoust. Soc. Amer.*, vol. 137, no. 3, pp. 1377–1388, Mar. 2015.



Chao Pan (SM'13) was born in 1989. He received the Bachelor degree in electronics and information engineering from the Northwestern Polytechnical University (NPU) in 2011. He is currently a Ph.D. student in information and communication engineering at NPU and also a visiting Ph.D. student at INRS-EMT, University of Quebec. His research interests are in speech enhancement, noise reduction, and microphone array signal processing for hands-free speech communications.



October 1995 to May 2003, he was first a Consultant and then a Member of the Technical Staff at Bell Laboratories, Murray Hill, NJ, USA. In May 2003, he joined the University of Quebec, INRS-EMT, in Montreal, Quebec, Canada, as a Professor. He is also a Visiting Professor at the Technion, Haifa, in Israel, an Adjunct Professor at Aalborg University, in Denmark, and a Guest Professor at Northwestern Polytechnical University, Xi'an, Shaanxi, in China.

His research interests are in signal processing, acoustic signal processing, and multimedia communications. He is the inventor of many important technologies. In particular, he was the lead researcher at Bell Labs who conceived and designed the world-first real-time hands-free full-duplex stereophonic teleconferencing system. Also, he conceived and designed the world-first PC-based multi-party hands-free full-duplex stereo conferencing system over IP networks.

He was the co-chair of the 1999 International Workshop on Acoustic Echo and Noise Control and the general co-chair of the 2009 IEEE Workshop on Applications of Signal Processing to Audio and Acoustics. He is the recipient, with Morgan and Sondhi, of the IEEE Signal Processing Society 2001 Best Paper Award. He is the recipient, with Chen, Huang, and Doclo, of the IEEE Signal Processing Society 2008 Best Paper Award. He is also the co-author of a paper for which Huang received the IEEE Signal Processing Society 2002 Young Author Best Paper Award. In 2010, he received the "Gheorghe Cartianu Award" from the Romanian Academy. In 2011, he received the Best Paper Award from the IEEE WASPAA for a paper that he co-authored with Chen.



Jingdong Chen (M'99–SM'09) received the Ph.D. degree in pattern recognition and intelligence control from the Chinese Academy of Sciences in 1998.

From 1998 to 1999, he was with ATR Interpreting Telecommunications Research Laboratories, Kyoto, Japan, where he conducted research on speech synthesis, speech analysis, as well as objective measurements for evaluating speech synthesis. He then joined the Griffith University, Brisbane, Australia, where he engaged in research on robust speech recognition and signal processing. From 2000 to

2001, he worked at ATR Spoken Language Translation Research Laboratories on robust speech recognition and speech enhancement. From 2001 to 2009, he was a Member of Technical Staff at Bell Laboratories, Murray Hill, New Jersey, working on acoustic signal processing for telecommunications. He subsequently joined WeVoice Inc. in New Jersey, serving as the Chief Scientist. He is currently a professor at the Northwestern Polytechnical University in Xi'an, China. His research interests include acoustic signal processing, adaptive signal processing, speech enhancement, adaptive noise/echo control, microphone array signal processing, signal separation, and speech communication.

Dr. Chen served as an Associate Editor of the IEEE TRANSACTIONS ON AUDIO, SPEECH, AND LANGUAGE PROCESSING from 2008 to 2014. He is currently a technical committee (TC) member of the IEEE Signal Processing Society (SPS) TC on Audio and Electroacoustics, and a member of the editorial advisory board of the *Open Signal Processing Journal*. He was the Technical Program Chair of IEEE TENCON 2013, a Technical Program Co-Chair of IEEE WASPAA 2009, IEEE ChinaSIP 2014, IEEE ICSPCC 2014, and IEEE ICSPCC 2015, and helped organize many other conferences. He co-authored the books *Design of Circular Differential Microphone Arrays* (Springer, 2015), *Study and Design of Differential Microphone Arrays* (Springer, 2013), *Speech Enhancement in the STFT Domain* (Springer, 2011), *Optimal Time-Domain Noise Reduction Filters: A Theoretical Study* (Springer, 2011), *Speech Enhancement in the Karhunen-Loève Expansion Domain* (Morgan&Claypool, 2011), *Noise Reduction in Speech Processing* (Springer, 2009), *Microphone Array Signal Processing* (Springer, 2008), and *Acoustic MIMO Signal Processing* (Springer, 2006).

Dr. Chen received the 2008 Best Paper Award from the IEEE Signal Processing Society (with Benesty, Huang, and Doclo), the best paper award from the IEEE Workshop on Applications of Signal Processing to Audio and Acoustics (WASPAA) in 2011 (with Benesty), the Bell Labs Role Model Teamwork Award twice, respectively, in 2009 and 2007, the NASA Tech Brief Award twice, respectively, in 2010 and 2009, the Young Author Best Paper Award from the 5th National Conference on Man-Machine Speech Communications in 1998. He was also a recipient of the Japan Trust International Research Grant from the Japan Key Technology Center in 1998 and the "Distinguished Young Scientists Fund" from the National Natural Science Foundation of China (NSFC) in 2014.